Clays and Clay Minerals, Vol. 69, No. 4:443–452, 2021

SUSTAINED ANTIBACTERIAL EFFECT OF LEVOFLOXACIN DRUG IN A POLYMER MATRIX BY HYBRIDIZATION WITH A LAYERED DOUBLE HYDROXIDE

Su-Joung Ko[1], Jin-Song Jung[2], Gyeong-Hyeon Gwak[3], Hyoung-Jun Kim[4], Fabrice Salles[5]*, and Jae-Min Oh[1]

[1]Department of Energy and Materials Engineering, Dongguk University-Seoul, Seoul 04620, Korea
[2]Department of Chemistry and Medical Chemistry, College of Science and Technology, Yonsei University, Wonju 26493, Republic of Korea
[3]Beamline Research Division, Pohang Accelerator Laboratory, Pohang University of Science and Technology, Pohang, Gyeongsangbukdo 37673, Republic of Korea
[4]Research Institute, National Cancer Center, 323 Ilsan-ro, Goyang, Gyeonggi 10408, Republic of Korea
[5]ICGM, University Montpellier, CNRS, ENSCM, Montpellier, France

Abstract—The immobilization of antimicrobial drugs can be used to expand the application of antibacterial properties to consumer products. The purpose of this study was to stabilize an antimicrobial agent, levofloxacin (LVX), for sustained antibacterial activity by immobilizing the drug molecules in a layered double hydroxide (LDH) and embedded in a polyurethane substrate. As-prepared MgAl-LDH was calcined at 400°C and reconstructed with LVX for intercalation. The X-ray diffraction patterns and cross-sectional transmission electron microscopy images showed lattice expansion along the crystallographic *c* axis upon LVX intercalation, suggesting successful loading of the drug. Fourier-transform infrared spectra revealed that the structure of LVX was well preserved between LDH layers. Elemental analysis indicated that the loading capacity of LVX in the hybrid was 41.7%. Bacterial-colony forming inhibitory assay on *Bacillus subtilis* exhibited ~100% antibacterial activity of both LVX alone and LVX-LDH hybrid (LL). To determine sustainability of antibacterial activity by the hybrid, either LVX alone or LL hybrid was loaded in the polyurethane (PU) substrate for which antibacterial activity was evaluated before and after immersion in a phosphate-buffered saline for 3 days. The LVX-composited PU showed a dramatic decrease in antibacterial activity, down to 0% after buffer treatment; LL-composited PU still contained antibacterial activity (~34% of colony suppression) after phosphate-buffered saline immersion.

Keywords—Antibacterial activity · Intercalation · Layered double hydroxide · Levofloxacin · Nanocomposite · Sustainability

INTRODUCTION

Bacterial infection remains a critical problem in biomedicine and presents a serious threat to human life (Hu et al., 2017). Studies have shown that bacteria attach to the surface of polymeric material and grow to form biofilms with the extracellular matrix, which is one of the essential causes of polymeric material contamination (Wang et al., 2016). Bacterial biofilms have antibiotic resistance that is several hundred times stronger than that of floating bacteria (Hoffman et al., 2005; Traba & Liang 2015). Infection by biofilms is becoming a potential risk factor in biomedical products such as catheters and implants, resulting in a critical threat to patients (Garcez et al., 2007; Conlon et al., 2013). An effective method of introducing antibiotics to biomedical devices to prevent potential infection is required, therefore.

Many researchers have tried to load antibiotics into medical polymers for antibacterial activity. Gentamicin-loaded silicone rubber has been developed to reduce infection on prosthetic heart valves in dogs (Olanoff et al., 1979). Gentamicin-incorporated poly(D,L-lactide) (PDLLA) coatings on titanium Kirschner wires reduced infection significantly in implants in rats (Lucke et al., 2003). The antibiotic-loaded polymeric matrix, however, released a burst of drug, resulting in the failure of long-term antibacterial activity (Ragel & Vallet-Regí, 2000; Hong et al., 2018). To control drug release from a polymer matrix, various strategies have been applied. For example, an antibiotic molecule was encapsulated in β-cyclodextrin and then grafted onto a polypropylene mesh for sustained efficacy for several days (Sanbhal et al., 2018). Antibiotics can be conjugated directly to polymers for sustained release of the drug and prolonged efficacy (Zhang et al., 2019). Sandwiching a drug between plasma-polymerized layers has been suggested as an alternative to controlled release of the drug from a solid carrier (Vasilev et al., 2011). Drugs can be immobilized in nanoparticles for this purpose, exemplified by a composite between polymer and antimicrobial drug-loaded nanoparticles (Pinto et al., 2011; Saha et al., 2014; Patel et al., 2016). In this strategy, nanomaterials were used as support for an antibiotic drug to immobilize it or delay its release (Pinto et al., 2011; Saha et al., 2014). As a support for antibacterial drugs, many inorganic materials such as zeolite (Khodaverdi et al., 2016), hydroxylapatite (Geuli et al., 2017), silica gel (Latifi et al., 2017), etc. are used. Among them, layered double hydroxide (LDH) is a fascinating candidate as a drug support. It consists of positively charged

This paper is based on a presentation made during the 4th Asian Clay Conference, Thailand, June 2020.

* E-mail address of corresponding authors: fabrice.salles@umontpellier.fr
DOI: 10.1007/s42860-021-00128-7

metal hydroxide layers and interlayer anions, with the general chemical formula $M(II)_{1-x}M(III)_x(OH)_2(A^{n-})_{x/n}\cdot mH_2O$ (M(II): divalent metal cation, M(III): trivalent metal cation, A^{n-}: interlayer anion, $0.2 < x < 0.4$) (Cavani et al., 1991; Rives, 2001). In terms of biomedical application, LDH has various advantages such as anion-exchange capacity, biocompatibility, controlled drug release, etc. (Choy et al., 1999, 2000; Senapati et al., 2016). Because LDH can incorporate and immobilize anionic antibacterial drugs in its gallery space, the drug-LDH loaded polymer composite would have sustained antibacterial activity through controlled release.

In the current study, a composite polyurethane (PU, as biocompatible polymer substrate) and levofloxacin (LVX, as an antibiotic)-intercalated LDH (as a support for antibiotic) was prepared in order to prolong antibacterial activity of LVX in polymeric material. It was hypothesized that LDH played a role as not only a LVX reservoir but also as mediator between drug and polymer. Because LVX is a water-soluble drug, direct coating or mixing of a drug moiety would not guarantee stabilized attachment on the polymer substrate. On the other hand, the encapsulation of LVX in LDH is considered to enhance the attachment efficiency toward a substrate and to provide the surface of the substrate with amounts of drug in a controlled manner. To achieve the strategy, LVX was incorporated into LDH, i.e. LL hybrid through reconstruction as previously reported (Kim et al., 2016a, 2016b). The long-term antibacterial activities of LL hybrid against *Bacillus subtilis* is demonstrated here.

EXPERIMENTAL

Material

Magnesium nitrate hexahydrate ($Mg(NO_3)_2\cdot 6H_2O$) and aluminum nitrate nonahydrate ($Al(NO_3)_2\cdot 9H_2O$) were purchased from Sigma Aldrich Co. LLC (St. Louis., Missouri, USA). Sodium hydroxide pellets (NaOH) and sodium bicarbonate ($NaHCO_3$) were obtained from Daejung Chemicals & Metals Co., Ltd. (Siheung, Korea). Levofloxacin ($C_{18}H_{20}FN_3O_4$) was acquired from Tokyo Chemical Industry Co., Ltd. (Tokyo, Japan). N-Methyl-2-pyrrolidone (NMP, C_4H_9NO) was obtained from Junsei Chemical Co., Ltd. (Tokyo, Japan). Polyurethane (PU) film was purchased from CY International Co., Ltd. (Seoul, Korea). All reagents were utilized without further purification.

Synthesis of Pristine LDH and Levofloxacin-intercalated LDH Nanohybrid

Pristine MgAl-LDH was prepared by conventional coprecipitation and consecutive hydrothermal treatment (Kim et al., 2018a, 2018b). A mixed-metal solution (0.3 mol/L $Mg(NO_3)_2\cdot 6H_2O$ and 0.15 mol/L $Al(NO_3)_2\cdot 9H_2O$) was titrated with an alkaline solution (0.9 mol/L NaOH and 0.675 mol/L $NaHCO_3$) until a pH of 9.5 was reached. The slurry obtained was transported to a teflon-lined autoclave bomb and then treated at 100°C for 48 h. The resulting white suspension was centrifuged, washed thoroughly with deionized water, and lyophilized. The pristine synthesized LDH powder was placed in an alumina boat and calcined under a muffle furnace at 400°C for 9 h with a heating rate of 0.8°C/min. The calcined LDH was designated as a layered double oxide (LDO). In order to prepare levofloxacin (LVX)-intercalated LDH hybrid (LL), powdered LVX was dispersed in deionized water (0.225 mol/L) and titrated with an alkaline solution (0.1 mol/L NaOH) until the pH reached ~10.0 for deprotonation. The LDO powder was added to the LVX solution with vigorous stirring under a N_2 atmosphere for 10 days. The stoichiometry between Al in LDO and LVX was set at 1.5. The product was collected by centrifugation (7,800×g, 5 min) and lyophilized.

Characterization of LL

The crystal structures of pristine LDH and the LL hybrid were investigated by powder XRD (using CuKα radiation) at the 8D XRS POSCO beamline, Pohang Accelerator Laboratory (PAL), Korea. The XRD patterns were measured in the range 1–30°2θ with a time step increment of 0.02°2θ and scanning rate of 0.5 s/step. The compositions of the metallic elements of the LL hybrid were analyzed by inductively coupled plasma-optical emission spectrometry (ICP-OES; OPTIMA 7300DV, Perkin Elmer, Waltham, Massachusetts, USA). The powdered sample was dissolved in hydrochloric acid which was evaporated on a hot plate. The remnant was diluted with 100 mL of deionized water and filtered with a syringe filter (PTFE, 0.45 μm, 13 mm, ADVANTEC®, Toyo Roshi Kaisha, Ltd, Tokyo, Japan) for ICP measurement. The loading capacity of LVX in the LL hybrid was quantified by CHNS elemental analysis (2400 Series II CHNS/O Analyzer, Perkin Elmer, Waltham, Massachusetts, USA). The intact structure of LVX in LL hybrid was evaluated by FTIR spectroscopy and the data analyzed using the software *Spectrum one* B.v5.0 (Perkin Elmer, Waltham, Massachusetts, USA). The FTIR spectra were obtained by the conventional KBr pellet method in the range 450 to 4000 cm^{-1}. The morphology and particle size of the prepared samples were confirmed by scanning electron microscopy (SEM) using a Quanta 250 FEG (FEI Company, Hillsboro, Oregon, USA). For the SEM measurement, the samples were dispersed in deionized water. Then the suspension was dropped onto a silicon wafer and dried. The surface of the specimen was sputtered with Pt/Pd for 60 s, and the images were obtained using a 30 kV accelerated electron beam. The cross-sectional morphology and interlayer distance of the LL hybrid were determined by Field Emission Transmission Electron Microscopy (FE-TEM; Titan G2 ChemiSTEM Cs probe, FEI company, Hillsboro, Oregon, USA) operated at an accelerating voltage of 200 kV. A powdered sample was fixed in Eponate 12 resin and slices of specimens for cross-sectional observation were prepared with a Cryo Ultramicrotome (CUMT; PT PC Ultramicrotome & Photographic, Boeckeler Instruments, Inc, Tucson, Arizona, USA).

Computational Section for DFT and Monte Carlo Simulations

In order to determine the molecular distribution of LVX ions in the LDH interlayer space, Monte Carlo simulations were performed using a homemade code.

https://doi.org/10.1007/s42860-021-00128-7 Published online by Cambridge University Press

The initial step consisted of determining the structure of LVX. It was built and optimized using density functional theory (DFT) calculations (with the code *DMol*^{3}). Then the partial charges were evaluated. For that purpose, optimization was performed using the GGA/PW91 functional combined with DNP basis set. Furthermore, all electrons were considered for the core treatment. The convergence parameters for energy, maximum force, and maximum force variation were 10^{-5} Ha (equivalent to 27.211×10^{-5} eV), 0.02 Ha/Å, and ±0.005 Ha/Å, respectively.

The structure of LDH was taken from the literature by modifying the chemical composition in order to be close to the experimental composition, while the simulated unit-cell parameters were fixed to those obtained experimentally. For the LDH structure, partial charges were calculated using the electronegativity equalization method. The Lennard-Jones parameters were issued from universal force field (UFF). A multi-cell formed by 3×3×1 unit cells for LDH was used for Monte Carlo calculations, in agreement with a fixed cut-off value for Lennard-Jones contributions of 12.5 Å. The Lorentz-Berthelot combining rule was used to determine the Lennard-Jones parameters for the adsorbate/adsorbent. For long-range electrostatic interactions, the Ewald summation technique was applied.

The simulations were performed in order to minimize the system energy by introducing a fixed number of ions in the structure. During these calculations, the motion of the ions included translation and rotation randomly considered during the equilibration steps. For that purpose, 2×10^7 Monte Carlo production steps following 2×10^7 equilibration steps were performed at 300 K to extract the maximum saturation in LVX (in agreement with the electrical neutrality of the solid and constituent ions) and the distribution of interlayer ions, as well as the snapshots illustrating the interaction between LVX and LDH layers and between two LVX layers.

Preparation of LVX-PU and LL-PU Composites

In order to prepare the LVX-PU and LL-PU composites, first, 1 g of PU film was cut into small pieces and placed in a vial. Then, 10 mL of NMP was added to the vial and stirred at 60°C for 4 h on a hot plate to melt the PU film completely. Then, LVX or LL powder was added to the PU solution with an equivalent LVX concentration of 5.0 mg/mL. The PU solution containing either LVX or LL powder was transferred to a 50 mL beaker. The PU solution was dried at 60°C on a hot plate for 3 days in a fume hood. Then, the LVX-PU or LL-PU composite was separated from the beaker using tweezers.

Release Study

Time-dependent release profiles of LVX from the LL hybrid were obtained in the following way. Hybrid powder (10 mg) was dispersed in 50 mL of saline media (JW Pharmaceutical Co., Ltd., Seoul, Korea). Aliquots (1 mL) were collected at determined time points, and then centrifuged at 8,000×g for 10 min and filtered with a syringe filter. The amount of LVX released in the supernatant was quantified using visible-light spectroscopy (Varioskan LUX multimode microplate reader, Thermo Fisher Scientific, Waltham, Massachusetts, USA) at a wavelength of 330 nm. Experiments were performed in triplicate.

The time-dependent release behavior of LVX was analyzed by various kinetic models, including a first-order equation (Eq. 1), the Elovich equation (Eq. 2), and the Power function (Eq. 3).

$$\ln Q_t = \ln Q_e - kt \quad (1)$$

where k is a first-order rate constant (h^{-1}).

$$Q_t = a + b\ln t \quad (2)$$

where a is the quantity released in the initial phase and b is the release rate.

$$Q_t = \alpha t^{\beta} \quad (3)$$

where α is a constant related to the initial desorption rate and β is the desorption rate coefficient.

Q_t is the amount released at time t (min) and Q_e is the amount released at equilibrium from all models.

Evaluation of Antibacterial Activity

LVX and LL Hybrid. The antibacterial activities of the LVX and LL hybrid were evaluated against the gram-positive bacterium *Bacillus subtilis* (*B. sub*) utilizing a colony-forming inhibitory assay. 0.5 mL of LVX solution or LL hybrid suspension with an equivalent LVX concentration of 1.0 ppm was mixed with 1.5 mL of the suspension containing 2.0×10^6 bacteria of *B. subtilis* and inoculated in an incubator at 37°C for 8 h. Then, the incubated bacteria suspension was collected, diluted to 1.0×10^3 bacteria/mL and spread on agar culture plates. The agar plates containing bacteria were incubated at 37°C for 12 h. The number of colonies was counted using a digital camera and a colony-counting program (Image Processing and Analysis in Java; *ImageJ*) to calculate antibacterial activity. All the antibacterial tests were run in triplicate.

LVX-PU and LL-PU Composite. The antibacterial activities of LVX- and LL-PU composites were also evaluated against *B. subtilis*, as above. Each composite was placed in a 45-mL conical tube and then sterilized with ultraviolet radiation for 30 min. The 1.5 mL suspension of *B. subtilis* (9.9×10^5 bacteria inside the suspension) was added to the tube containing the composite and inoculated at 37°C for 3 days. The conical tube without composite was used as a control. The antibacterial activity was then determined using the colony-forming inhibition assay as described above. All tests were run in triplicate.

In order to examine the sustained antibacterial activity after exposure to physiological aqueous conditions, each composite was immersed in phosphate-buffered saline (PBS, pH 7.4±0.1, WELGENE Inc, Gyeongsan, Korea) and kept at room temperature for 3 days. The surface of the composite was rinsed with deionized water to remove any released antibiotic, and dried at 60°C for 5 h. Then the antibacterial activity of composite was

https://doi.org/10.1007/s42860-021-00128-7 Published online by Cambridge University Press

subjected to the colony-forming inhibition assay as described above.

RESULTS AND DICUSSION

XRD

The XRD patterns of pristine LDH (Fig. 1Aa) revealed sharp characteristic peaks for hydrotalcite (JCPDS card No. 14-0191) as (003), (006), (012), (015), and (018) at 11.7, 23.5, 34.9, 41.7, and 45.5°2θ, respectively (Oh et al., 2002; Wiyantoko et al., 2015). The d_{003} value of pristine LDH was 0.76 nm, corresponding to carbonate anions in the interlayer (Oh et al., 2002). Calcined LDH, i.e. LDO, showed diffraction peaks at 35.2 and 43.2°2θ, corresponding to (111) and (200) of periclase (JCPDS card No. 71-1176) (Fig. 1Ab). The XRD patterns of LL hybrid (Fig. 1Ac) exhibited a (003) peak at 2.82°2θ, a (009) peak at 8.46°2θ, and a (012) peak at 34.9°2θ. The (00l) peak shift to a lower angle indicated that intercalation of larger molecules into LDH; the d_{003} spacing of LDH increased from 0.76 nm to 3.13 nm upon intercalation of LVX. Preservation of the (012) peak at 34.9°2θ indicated that no significant lattice deterioration occurred upon intercalation of LVX through reconstruction. Small peaks of (003) and (006) corresponding to a d_{003} spacing of 0.76 nm were observed in the XRD pattern for LL, suggesting the potential existence of CO_3^{2-}. During the reconstruction process, some of the LDO particles underwent reconstruction with carbonate rather than with LVX.

The interlayer arrangement of LVX molecules in LDH is proposed in Fig. 1B based on Monte Carlo simulation starting from XRD data. The main interactions were electrostatic attraction between the negative charge of LVX and the positive LDH layer (Fig. 1Bc) with a spacing of ~2.1 Å. Furthermore, the LVX molecules interacted with each other through π-π stacking with an intermolecular distance of ~4.2 Å (Fig. 1Bd).

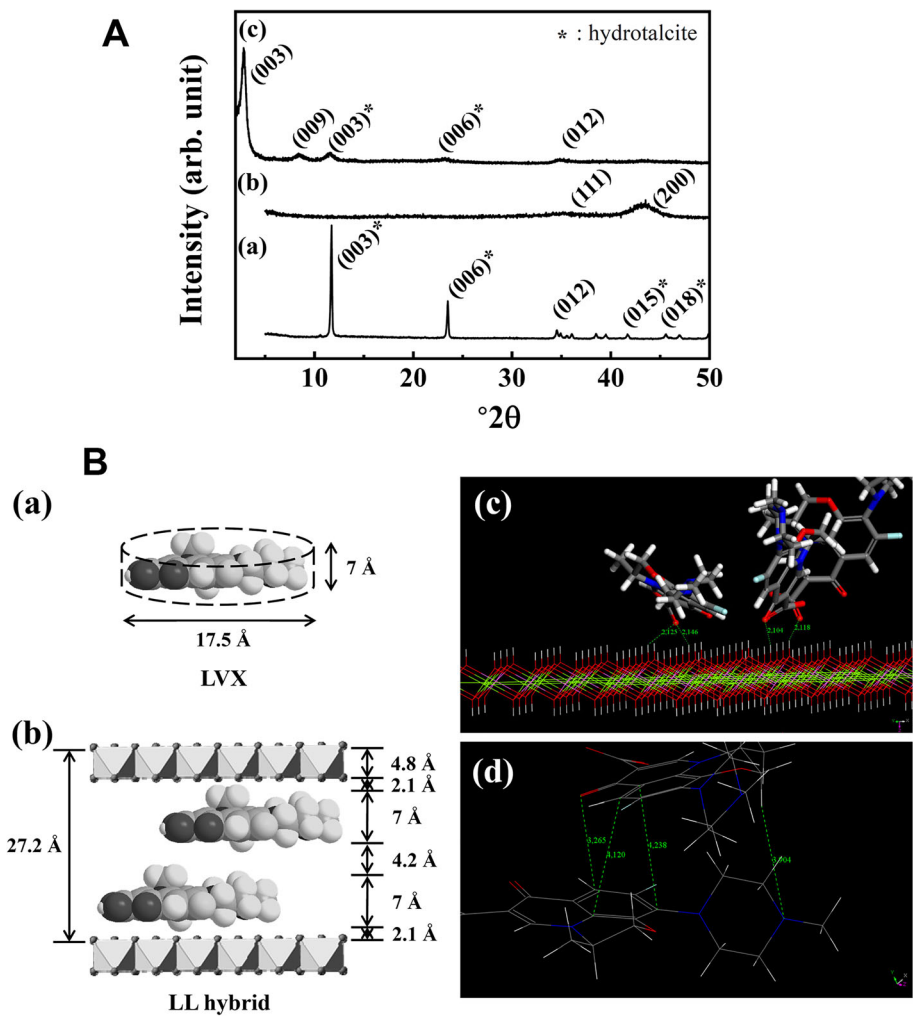

Fig. 1. A XRD patterns for **a** pristine LDH, **b** LDO, and **c** LL hybrids. **B a** Schematic dimensions of LVX, **b** proposed interlayer arrangement of LL hybrid, **c** main interactions between LVX and LDH layer extracted from Monte Carlo simulations, and **d** illustration of the π-stacking effect between LVX in the interlayer space, extracted from Monte Carlo simulations

https://doi.org/10.1007/s42860-021-00128-7 Published online by Cambridge University Press

Taking into account the theoretical values for molecular thickness of LVX (~7 Å), intermolecular distance (~4.2 Å), LVX-LDH distance (~2.1 Å), and layer thickness of LDH (~4.8 Å), the bilayer model of LVX molecules with parallel orientation was considered the most plausible interlayer structure (Fig. 1Bb). The dual stabilization of LVX through electrostatic interaction and intermolecular π-π interaction was considered advantageous for immobilizing drug moieties in a LDH matrix.

The crystallinity along the crystallographic *c*-axis direction was calculated by Scherrer's equation as follows: $t = (0.9\lambda)/(B\cdot\cos\theta)$, where t = crystallite size, λ = X-ray wavelength, B = full-width-at-half-maximum, and θ = Bragg angle (Culity & Stock 1978). The crystallite size along the (003) plane decreased from 55.4 nm to 16.1 nm after hybridization. The reduced crystallite size was attributed to random stacking between LDH layers and organic moieties during reconstruction as reported previously (Kim et al,. 2016a).

FTIR

The chemical properties of LVX in the LL hybrid were confirmed through FTIR spectra. The IR spectrum of pristine LDH (Fig. 2a) exhibited characteristic peaks of CO_3^{2-} stretching vibrations and M–O vibrations in hydroxide layers at 1370 and 800 cm^{-1}, respectively (Kim et al., 2011). The spectrum of LVX (Fig. 2b) showed characteristic peaks for carboxyl C=O at 1725 cm^{-1}, for amines at 1294 cm^{-1}, and for C–F at 1087 cm^{-1} (Mouzam et al., 2011; Jalvandi et al., 2017; Nazar et al., 2017). After hybridization between pristine LDH and LVX through reconstruction, the amine and C–F stretching vibration of LVX and M–O vibration of hydroxyl layers were well preserved, suggesting that the structure of the drug inside the LL hybrid was intact (Fig. 2c). Note that, after hybridization, the peak for carboxyl C=O disappeared and new peaks corresponding to antisymmetric and symmetric stretching vibration of COO^- occurred at 1582 and 1400 cm^{-1} (Sultana et al., 2013; Al-Hussaini et al., 2018), respectively.

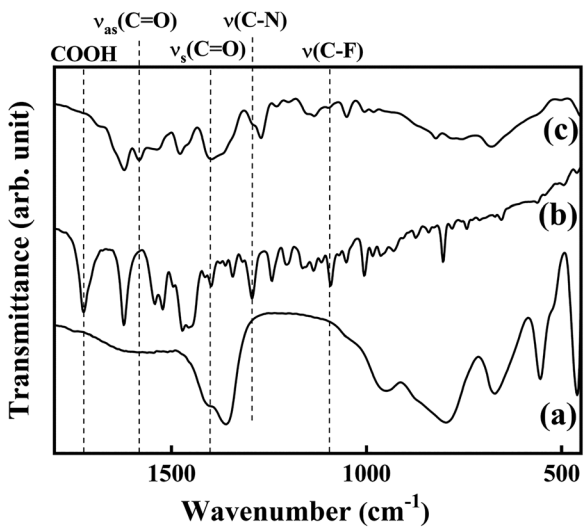

Fig. 2. Fourier-transform infrared spectra for **a** LDH, **b** LVX, and **c** LL

The results revealed that carboxylic acid in LVX was deprotonated to allow stabilization in LDH through electrostatic interaction. The XRD patterns and IR spectra of pristine LDH and LL hybrid suggested that LVX was intercalated successfully into the interlayer space of LDH by the reconstruction route.

Chemical Formula

The chemical formula of the LL hybrid, as determined from ICP-OES and elemental analyses, was $[Mg_{0.69}Al_{0.31}(OH)_2]^{0.31+}[(OH)_{0.10}(LVX)_{0.13}(CO_3)_{0.04}]^{0.31-}\cdot 0.1H_2O$. The calculated Mg:Al ratio of the metal hydroxide layer in the LL hybrid was 0.69:0.31 (25.62% of C content and 4.9% for N content). Although the chemical formula contained three anionic species in the second square brackets, it did not mean the co-intercalation of three species. As discussed in the XRD section, some LDO was considered to be reconstructed to a carbonate-LDH phase while most LDO transformed to LVX-intercalated LDH. The LVX content in the LL hybrid (loading capacity) was determined to be 41.7% from the chemical formula of LL hybrid, and this was fairly comparable with the theoretical loading. Considering the previous literature on drug-LDH hybrids (Oh et al., 2006; Kong et al., 2010), the LVX content in the LL hybrid was sufficiently high to achieve drug efficacy and the existence of carbonate is not expected to have a negative effect on its antibacterial performance.

SEM

The particle size and morphology of pristine LDH and LL hybrid were observed using scanning electron microscopy. The SEM image of pristine LDH (Fig. 3a) showed the typical coin-like shape of LDH with average particle size 265 ± 42 nm. After hybridization with LVX by reconstruction, the morphology of LDH changed to sand-rose shape which was formed by agglomeration of partially bent and thin layers (Fig. 3b) (Kang et al., 2015; Kim et al., 2018a). This result matched with previous studies which demonstrated the formation of sand-rose morphology for organic-LDH hybrids, resulting in partial delamination and increasing face-to-edge interaction during the reconstruction process (Kim et al., 2018a).

TEM

The cross-sectional TEM images (Fig. 4) showed the characteristic layered structure of LDH and revealed the expanded interlayer distance due to the intercalation of LVX. The interlayer distance of the LL corresponding to the periodic lattice fringe was confirmed to be 3.2 nm, and this value was in good agreement with the d_{003} value of the LL hybrid (3.13 nm) in the XRD pattern (Fig. 1Ab). In addition, the energy dispersive spectroscopy (EDS) mapping for the LL hybrid (Fig. 5) showed that the particles were composed mainly of Mg and Al forming the LDH plate. Homogeneous distribution of N and F was attributed to a LVX moiety which was mixed with the LDH lattice at the nanometer scale. The results supported the view that the LVX molecules were intercalated between LDH layers with notable periodic arrangement.

https://doi.org/10.1007/s42860-021-00128-7 Published online by Cambridge University Press

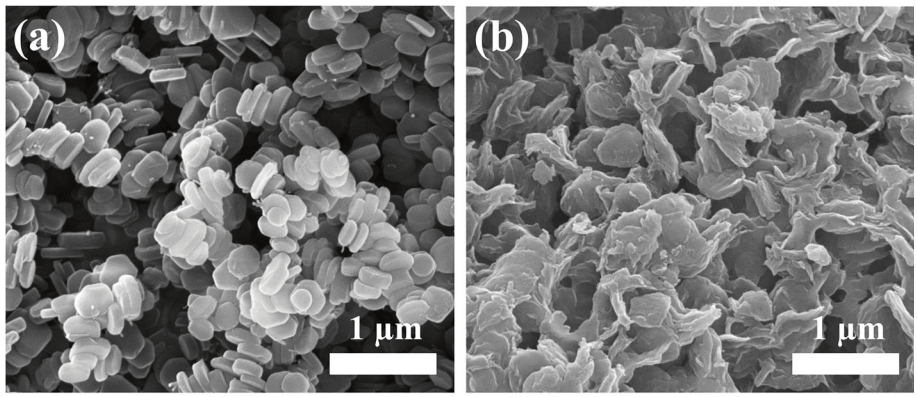

Fig. 3. SEM images for **a** pristine LDH and **b** LL hybrid

SEM Images of LVX and LL Hybrid-containing Composites

The SEM images of polyurethane (PU) after LVX or LL hybrid loading are shown in Fig. 6. LVX-loaded PU composite (Fig. 6a) exhibited the typical morphology of polymer material with a smooth surface. On the other hand, the SEM image of LL hybrid-loaded PU showed particle-like morphology out of the polymer matrix, which was attributed to the partially exposed LL hybrid. The inorganic part, LDH, of the LL hybrid is expected to protect LVX from abrupt release from the polymer matrix.

LVX Release Study from LL Hybrid

The LVX release in aqueous media (saline) from LL hybrid was tested in a time-dependent manner. As shown in Fig. 7, the fractional release of LVX consisted of a burst in the initial stage (~5 min) followed by sustained release, which corresponded to the typical release pattern of drug-intercalated LDH (Gu et al., 2008; Senapati et al., 2016). In order to interpret the release kinetics, the profile was fitted to three representative models: first-order, the Elovich model, and a power function, according to Eqs. 1–3.

According to the literature, the three models hypothesize the release condition as follows. First-order describes the release behavior mediated mainly by dissolution (bin Hussein et al., 2002); the Elovich model explains a release process through bulk surface diffusion (Senapati et al., 2016); the power function hypothesizes release by diffusion from flat surfaces or ion-exchange phenomena (Kang et al., 2015). The linear fitting yielded R^2 values of 0.786, 0.973, and 0.981 for first-order, Elovich, and power function models, respectively, suggesting that the release of LVX was best described by a power function model, which hypothesized release of molecules through a flat surface. In other words, the host LDH lattice played an important role in release control. The LL hybrid embedded in PU substrate was, therefore, expected to release LVX in a restricted manner due to the action of a flat LDH layer.

Antibacterial Activity of LVX and the LL Hybrid

In order to compare the antibacterial activity of LVX-PU and LL-PU composites, a bacterial-colony-forming inhibition assay was carried out against *B. subtilis*. For the first step, the antibacterial activities of LVX and LL hybrid were compared.

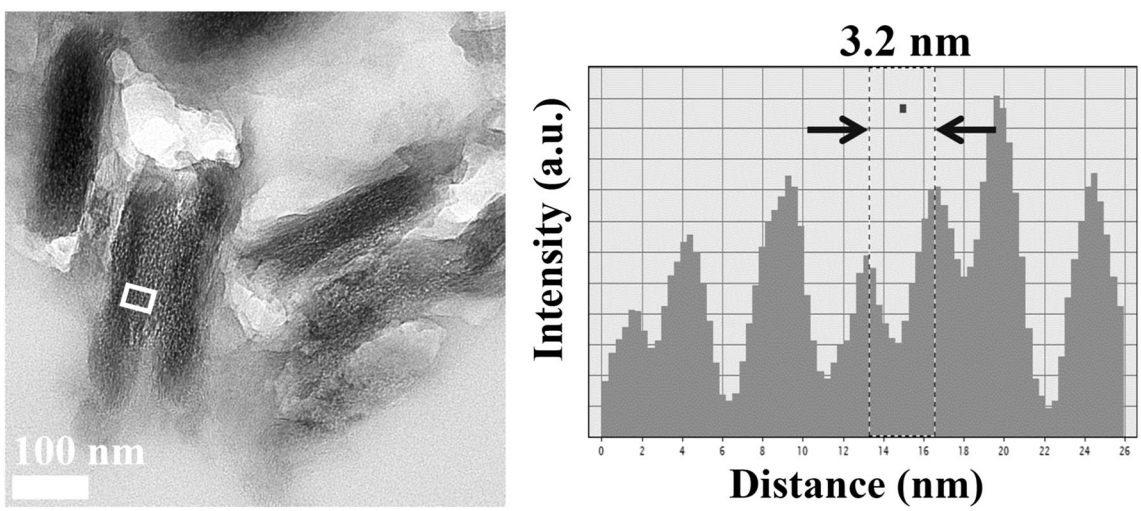

Fig. 4. Cross-sectional TEM image with histogram along the 00l direction for the LL hybrid

https://doi.org/10.1007/s42860-021-00128-7 Published online by Cambridge University Press

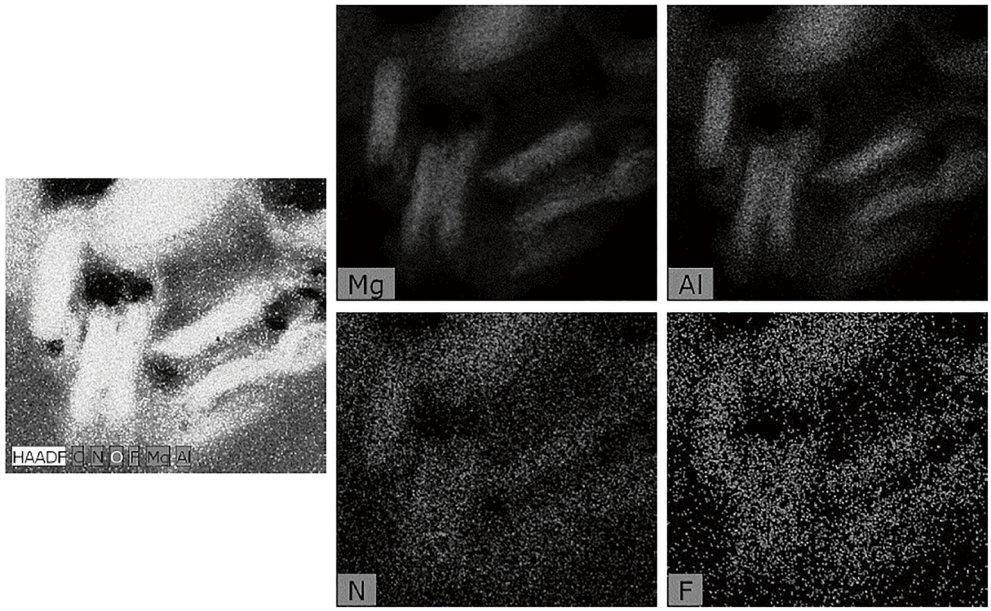

Fig. 5. Energy dispersive spectroscopy (EDS) mapping for LL hybrid

As a preliminary study, both samples with 0.5, 1.0, and 2.5 ppm of drug concentration were treated to the bacteria, and 1.0 ppm was selected as the minimum concentration point to show 100% antibacterial activity. Note that LL hybrid, which contained a drug moiety within its interlayer space, showed the same antibacterial activity with LVX at a drug concentration of 1.0 ppm (Fig. 8). According to a previous study (Al-Hussaini et al., 2018), LVX and LVX-intercalated LDH exhibited antibiotic inhibition zones in a paper disc assay above a concentration of 5 ppm. In the research of Al-Hussaini et al., (2018), LVX-LDH had a smaller antibacterial effect than LVX alone. Although the previous data from paper disc assays cannot be compared directly with the current colony-forming assay, the current LL hybrid could be considered to have a comparable antibacterial effect to LVX alone at a reasonably low concentration. The antibacterial effectiveness of the LL hybrid was ascribed to the concentrated drug release at the interface between LL particles and microbes. Unlike LVX solution, where the LVX concentration was uniform throughout, the LL hybrid had a heterogeneous concentration distribution — the LVX moiety converged on LL particles. Thus, LL particles could exhibit a significant bactericidal effect if they encountered microbes.

Next, the antibacterial activities of LVX-PU and LL-PU composites containing 5.0 mg of LVX per 1.0 g of composite were evaluated (Fig. 9). The LVX-PU and LL-PU composites showed 100% antibacterial activity against *B. subtilis,* as expected from the efficacy of the material itself. This could be expected from the large antibacterial effect of both LVX and LL (Fig. 8). Microbes attached to the surfaces of films would be influenced readily by the drug moiety which was exposed at the composite surface or partially released from inside the

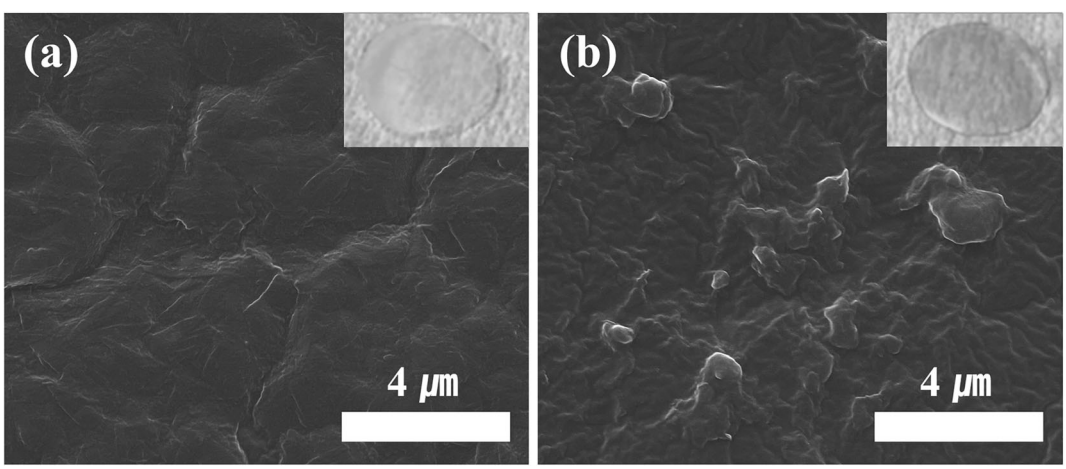

Fig. 6. SEM images for the surface of **a** LVX-PU and **b** LL-PU composite. Inset is a photograph of each sample

https://doi.org/10.1007/s42860-021-00128-7 Published online by Cambridge University Press

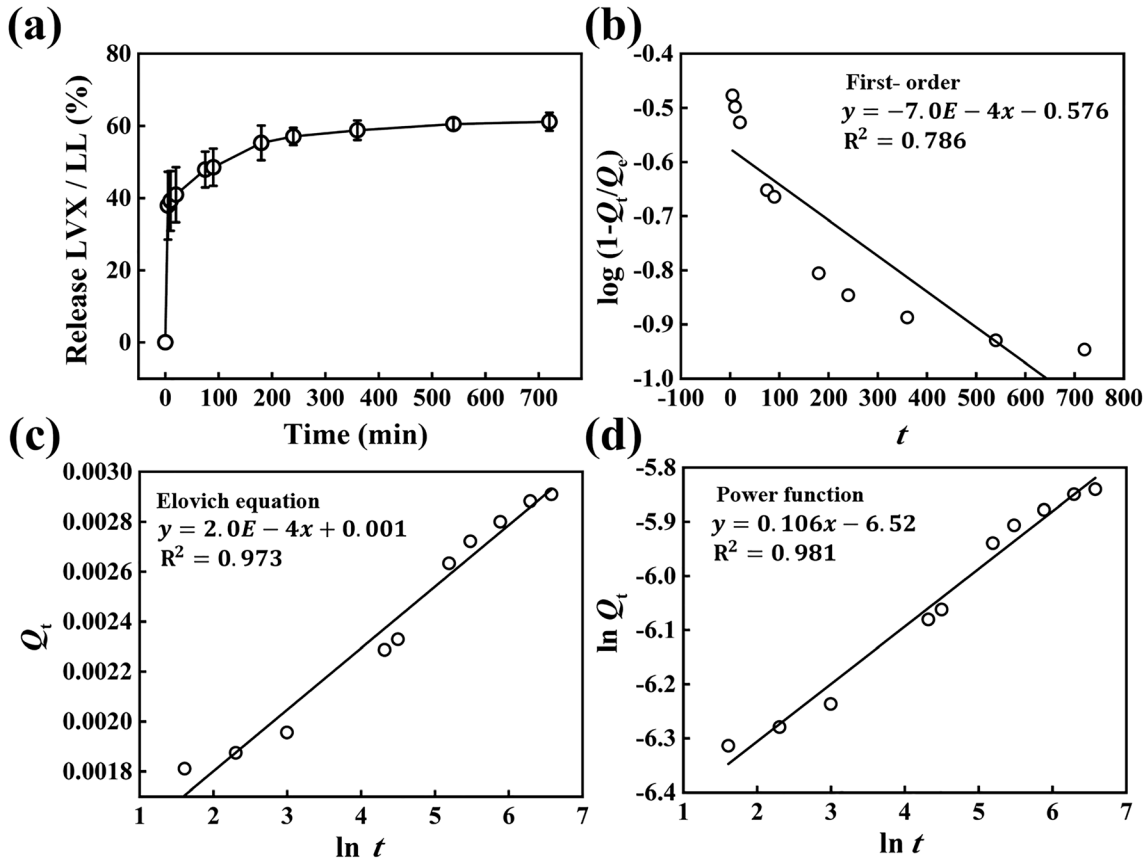

Fig. 7. a Time-dependent LVX release from the LL hybrid in saline media. Analyses of release kinetics with **b** first-order equation, **c** Elovich equation, and **d** power function

composite. This kind of ready antibacterial action might well diminish when the material is placed for prolonged periods in aqueous conditions, e.g. in an implanted device or in a liquid flowing through a medical tube. In order to control the release

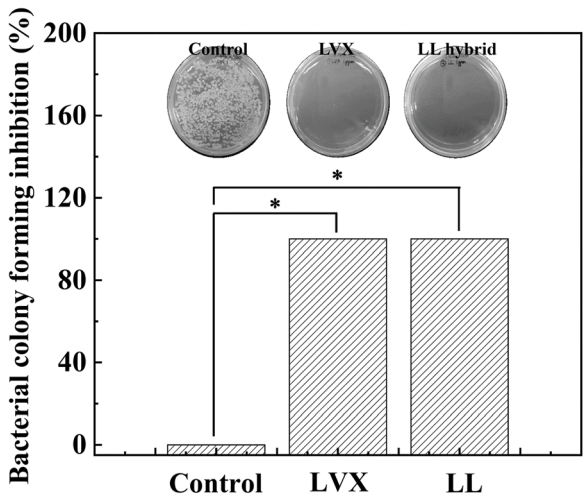

Fig. 8. Bacterial colony forming (%) of LVX solution and LL hybrid suspension on *Bacillus subtilis*. The asterisk indicates the statistical equivalence and difference with confidence intervals of 100% calculated by Student's *t*-test

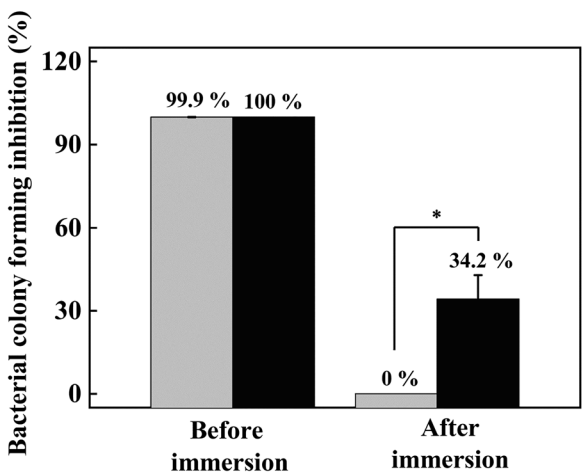

Fig. 9. Bacterial colony-forming inhibition (%) of LVX-PU (gray bar) and LL-PU (black bar) composites against *Bacillus subtilis*. Both composites were immersed in phosphate-buffered saline simulating biological conditions. The asterisk indicates statistical difference in the 99.5% confidence interval

https://doi.org/10.1007/s42860-021-00128-7 Published online by Cambridge University Press

of antibiotics from a solid substrate, various methods have been suggested, e.g. LVX sandwiched by plasma polymerized layers on a solid substrate to control release depending on layer-thickness (Vasilev et al. 2011). Approximately 50% of drug release was shown to be suppressed within 30 h under PBS conditions (Vasilev et al., 2011). In another approach, LVX was first encapsulated by β-cyclodextrin which was further grafted onto a polypropylene-based medical mesh which showed sustained antibacterial efficacy for 7 days (Sanbhal et al., 2018). Antibacterial material could be conjugated directly with polymers for dental implant application (Zhang et al., 2019), where sustained release of the drug was observed for 25 days under PBS conditions. Similarly to previous studies, the current system was designed to retard release of the embedded drug. The immersion of both composites in PBS for 3 days changed dramatically the antibacterial efficacy of the materials. The antibacterial activity of the LVX-PU composite decreased to 0% upon PBS immersion; on the other hand, the antibacterial activity of the LL-PU composite remained, showing ~34% of colony-forming inhibition. From the antibacterial activity of LVX-PU and LL-PU composites before and after immersion in PBS for 3 days, LL-PU composites were confirmed to have sustained antibacterial activity compared to LVX-PU in physiological conditions. Water-soluble drugs such as LVX can be washed easily from the polymer substrate when placed under aqueous conditions. A composite was prepared using bioactive glass, biopolymer, and a water-soluble drug, gentamicin (Ragel & Vallet-Regí, 2000). Due to its significant solubility in water, 80% of the drug was released readily from the composite within 1 day in a physiological solution. Current LVX-PU composites would undergo a similar process of fast release. As expected from the release section, however, the release of LVX in LL hybrid was controlled by the surface of LDH layers, and thus more steps would be required for LVX molecules to escape from the composite. In this way, the LL-PU composite is considered to suppress drug release and to prolong antibacterial effects under aqueous conditions.

CONCLUSIONS

An LVX-LDH hybrid was prepared by reconstruction to immobilize an antibiotic in a composite and to examine sustained antibacterial activity of the polymer containing the hybrid. The XRD patterns and FTIR spectra of pristine LDH and LL hybrid showed that LVX was intercalated successfully into the interlayer space of the LDH by the reconstruction route. According to ICP-OES and elemental analysis, the hybrid was found to have 41.7% of LVX loading capacity. The SEM images of pristine LDH and LL hybrid showed that the coin-like shape of pristine LDH with a 265±42 nm particle size was changed to sand-rose shape with a heterogeneous particle size, which was a typical pattern found in reconstruction. From cross-sectional TEM analysis with EDS mapping, the interlayer distance of LL hybrids was shown to match the d_{003} value from XRD patterns, ~3.2 nm, and the composition of metal layer (Mg and Al) and LVX (N and F) was well distributed throughout the LL hybrid. Both LVX-PU and LL-PU composites showed 100% antibacterial activity against *B. subtilis* as prepared. After immersion in PBS for 3 days, however, the antibacterial activity of LVX-PU composite reduced to 0%, while the LL-PU composite maintained ~34% antibacterial activity.

ACKNOWLEDGMENT

This work was supported by the Dongguk University Research Fund of 2019.

FUNDING

Funding sources are as stated in the Acknowledgments.

Declarations

Conflict of Interest

The authors declare that they have no conflict of interest.

REFERENCE

Al-Hussaini, S., Al-Ghanimi, A., & Kadhim, H. J. S. J. M. R. (2018). Preparation of nanohybrid antibiotic from levofloxacin and determination its inhibitory efficacy against staphylococcus aureus isolated from diabetic foot ulcer. *Scientific Journal of Medical Research, 2*, 29–35.

Bin Hussein, M. Z., Zainal, Z., Yahaya, A. H., & Foo, D. W. V. (2002). Controlled release of a plant growth regulator, α-naphthaleneacetate from the lamella of Zn-Al-layered double hydroxide nanocomposite. *Journal of Controlled Release, 82*, 417–427.

Cavani, F., Trifirò, F., & Vaccari, A. (1991). Hydrotalcite-type anionic clays: Preparation, properties and applications. *Catalysis Today, 11*, 173–301.

Choy, J.-H., Kwak, S.-Y., Park, J.-S., Jeong, Y.-J., & Portier, J. (1999). Intercalative nanohybrids of nucleoside monophosphates and DNA in layered metal hydroxide. *Journal of the American Chemical Society, 121*, 1399–1400.

Choy, J.-H., Kwak, S.-Y., Jeong, Y.-J., & Park, J.-S. (2000). Inorganic layered double hydroxides as nonviral vectors. *Angewandte Chemie International Edition, 39*, 4041–4045.

Conlon, B. P., Nakayasu, E. S., Fleck, L. E., LaFleur, M. D., Isabella, V. M., Coleman, K., Leonard, S. N., Smith, R. D., Adkins, J. N., & Lewis, K. (2013). Activated clpp kills persisters and eradicates a chronic biofilm infection. *Nature, 503*, 365–370.

Culity, B. D., & Stock, S. R. (1978). *Elements of X-ray Diffraction* (2nd ed.). Pearson.

Garcez, A. S., Ribeiro, M. S., Tegos, G. P., Núñez, S. C., Jorge, A. O. C., & Hamblin, M. R. (2007). Antimicrobial photodynamic therapy combined with conventional endodontic treatment to eliminate root canal biofilm infection. *Lasers in Surgery and Medicine, 39*, 59–66.

Geuli, O., Metoki, N., Zada, T., Reches, M., Eliaz, N., & Mandler, D. (2017). Synthesis, coating, and drug-release of hydroxyapatite nanoparticles loaded with antibiotics. *Journal of Materials Chemistry B, 5*, 7819–7830.

Gu, Z., Thomas, A. C., Xu, Z. P., Campbell, J. H., & Lu, G. Q. (2008). In vitro sustained release of LMWH from MgAl-layered double hydroxide nanohybrids. *Chemistry of Materials, 20*, 3715–3722.

Hoffman, L. R., D'Argenio, D. A., MacCoss, M. J., Zhang, Z., Jones, R. A., & Miller, S. I. (2005). Aminoglycoside antibiotics induce bacterial biofilm formation. *Nature, 436*, 1171–1175.

Hong, Y., Xi, Y., Zhang, J., Wang, D., Zhang, H., Yan, N., He, S., & Du, J. (2018). Polymersome–hydrogel composites with combined

https://doi.org/10.1007/s42860-021-00128-7 Published online by Cambridge University Press

quick and long-term antibacterial activities. *Journal of Materials Chemistry B, 6*, 6311–6321.

Hu, J., Quan, Y., Lai, Y., Zheng, Z., Hu, Z., Wang, X., Dai, T., Zhang, Q., & Cheng, Y. (2017). A smart aminoglycoside hydrogel with tunable gel degradation, on-demand drug release, and high antibacterial activity. *Journal of Controlled Release, 247*, 145–152.

Jalvandi, J., White, M., Gao, Y., Truong, Y. B., Padhye, R., & Kyratzis, I. L. (2017). Polyvinyl alcohol composite nanofibres containing conjugated levofloxacin-chitosan for controlled drug release. *Materials Science and Engineering: C, 73*, 440–446.

Kang, H., Kim, H.-J., Yang, J.-H., Kim, T.-H., Choi, G., Paek, S.-M., Choi, A.-J., Choy, J.-H., & Oh, J.-M. (2015). Intracrystalline structure and release pattern of ferulic acid intercalated into layered double hydroxide through various synthesis routes. *Applied Clay Science, 112–113*, 32–39.

Khodaverdi, E., Soleimani, H. A., Mohammadpour, F., & Hadizadeh, F. (2016). Synthetic zeolites as controlled-release delivery systems for anti-inflammatory drugs. *Chemical Biology & Drug Design, 87*, 849–857.

Kim, K.-M., Park, C.-B., Choi, A.-J., Choi, H.-J., & Oh, J.-M. (2011). Selective DNA adsorption on layered double hydroxide nanoparticles. *Bulletin of the Korean Chemical Society, 32*, 2217–2221.

Kim, H.-J., Kim, T.-H., Kim, H.-M., Hong, I.-K., Kim, E.-J., Choi, A.-J., Choi, H.-J., & Oh, J.-M. (2016a). Nano-biohybrids of engineered nanoclays and natural extract for antibacterial agents. *Applied Clay Science, 134*, 19–25.

Kim, T.-H., Kim, H.-J., Choi, A.-J., Choi, H.-J., & Oh, J.-M. (2016b). Hybridization between natural extract of Angelica gigas akai and inorganic nanomaterial of layered double hydroxide via reconstruction reaction. *Journal of Nanoscience and Nanotechnology, 16*, 1138–1145.

Kim, H.-J., Lee, G. J., Choi, A.-J., Kim, T.-H., & Kim, T.-i., & Oh, J.-M. (2018a). Layered double hydroxide nanomaterials encapsulating *Angelica gigas* nakai extract for potential anticancer nanomedicine. *Frontiers in Pharmacology, 9*, 723. https://doi.org/10.3389/fphar.2018.00723.

Kim, T.-H., Hong, I. T., & Oh, J.-M. (2018b). Size- and surface charge-controlled layered double hydroxides for efficient algal flocculation. *Environmental Science: Nano, 5*, 183–190.

Kong, X., Jin, L., Wei, M., & Duan, X. (2010). Antioxidant drugs intercalated into layered double hydroxide: Structure and in vitro release. *Applied Clay Science, 49*, 324–329.

Latifi, L., Sohrabnezhad, S., & Hadavi, M. (2017). Mesoporous silica as a support for poorly soluble drug: Influence of ph and amino group on the drug release. *Microporous and Mesoporous Materials, 250*, 148–157.

Lucke, M., Schmidmaier, G., Sadoni, S., Wildemann, B., Schiller, R., Haas, N. P., & Raschke, M. (2003). Gentamicin coating of metallic implants reduces implant-related osteomyelitis in rats. *Bone, 32*, 521–531.

Mouzam, M. I., Dehghan, M. H. G., Asif, S., Sahuji, T., & Chudiwal, P. (2011). Preparation of a novel floating ring capsule-type dosage form for stomach specific delivery. *Saudi Pharmaceutical Journal, 19*, 85–93.

Nazar, M. F., Saleem, M. A., Bajwa, S. N., Yameen, B., Ashfaq, M., Zafar, M. N., & Zubair, M. (2017). Encapsulation of antibiotic levofloxacin in biocompatible microemulsion formulation: Insights from microstructure analysis. *The Journal of Physical Chemistry B, 121*, 437–443.

Oh, J.-M., Hwang, S.-H., & Choy, J.-H. (2002). The effect of synthetic conditions on tailoring the size of hydrotalcite particles. *Solid State Ionics, 151*, 285–291.

Oh, J.-M., Park, M., Kim, S.-T., Jung, J.-Y., Kang, Y.-G., & Choy, J.-H. (2006). Efficient delivery of anticancer drug MTX through MTX-LDH nanohybrid system. *Journal of Physics and Chemistry of Solids, 67*, 1024–1027.

Olanoff, L. S., Anderson, J. M., & Jones, R. D. (1979). Sustained release of gentamicin from prosthetic heart valves. *ASAIO Journal, 25*, 334–338.

Patel, D. K., Biswas, A., & Maiti, P. (2016). 6-nanoparticle-induced phenomena in polyurethanes. In S. L. Cooper & J. Guan (Eds.), *Advances in Polyurethane Biomaterials* (pp. 171–194). Woodhead Publishing (an Elsevier imprint, Amsterdam).

Pinto, F. C. H., Silva-Cunha, A., Pianetti, G. A., Ayres, E., Oréfice, R. L., & Da Silva, G. R. (2011). Montmorillonite clay-based polyurethane nanocomposite as local triamcinolone acetonide delivery system. *Journal of Nanomaterials, 2011*, 1–11.

Ragel, C. V., & Vallet-Regí, M. (2000). In vitro bioactivity and gentamicin release from glass–polymer–antibiotic composites. *Journal of Biomedical Materials Research, 51*, 424–429.

Rives, V. (2001). *Layered Double Hydroxides: Present and Future*. Nova Publishers.

Saha, K., Butola, B. S., & Joshi, M. (2014). Drug release behavior of polyurethane/clay nanocomposite: Film vs. Nanofibrous web. *Journal of Applied Polymer Science, 131*, 40824.

Sanbhal, N., Saitaer, X., Li, Y., Mao, Y., Zou, T., Sun, G., & Wang, L. J. P. (2018). Controlled levofloxacin release and antibacterial properties of β-cyclodextrins-grafted polypropylene mesh devices for hernia repair. *Polymers (Basel), 10*, 493.

Senapati, S., Thakur, R., Verma, S. P., Duggal, S., Mishra, D. P., Das, P., Shripathi, T., Kumar, M., Rana, D., & Maiti, P. (2016). Layered double hydroxides as effective carrier for anticancer drugs and tailoring of release rate through interlayer anions. *Journal of Controlled Release, 224*, 186–198.

Sultana, N., Arayne, M. S., Rizvi, S. B. S., Haroon, U., & Mesaik, M. A. (2013). Synthesis, spectroscopic, and biological evaluation of some levofloxacin metal complexes. *Medicinal Chemistry Research, 22*, 1371–1377.

Traba, C., & Liang, J. F. (2015). Bacteria responsive antibacterial surfaces for indwelling device infections. *Journal of Controlled Release, 198*, 18–25.

Vasilev, K., Poulter, N., Martinek, P., & Griesser, H. J. (2011). Controlled release of levofloxacin sandwiched between two plasma polymerized layers on a solid carrier. *ACS Applied Materials & Interfaces, 3*, 4831–4836.

Wang, C.-H., Hou, G.-G., Du, Z.-Z., Cong, W., Sun, J.-F., Xu, Y.-Y., & Liu, W.-S. (2016). Synthesis, characterization and antibacterial properties of polyurethane material functionalized with quaternary ammonium salt. *Polymer Journal, 48*, 259–265.

Wiyantoko, B., Kurniawati, P., Purbaningtias, T. E., & Fatimah, I. (2015). Synthesis and characterization of hydrotalcite at different Mg/Al molar ratios. *Procedia Chemistry, 17*, 21–26.

Zhang, R., Jones, M. M., Moussa, H., Keskar, M., Huo, N., Zhang, Z., Visser, M. B., Sabatini, C., Swihart, M. T., & Cheng, C. (2019). Polymer–antibiotic conjugates as antibacterial additives in dental resins. *Biomaterials Science, 7*, 287–295.

(Received 9 September 2020; revised 4 April 2021; AE: Jinwook Kim)